JACS
JOURNAL OF THE AMERICAN CHEMICAL SOCIETY
Communication
pubs.acs.org/JACS

Half-Metallic Ferromagnetism in Synthetic Co_9Se_8 Nanosheets with Atomic Thickness

Xiaodong Zhang,[†] Jiajia Zhang,[†] Jinyang Zhao,[†] Bicai Pan,[†] Mingguang Kong,[‡] Jing Chen,[§] and Yi Xie*[,†]

[†]Hefei National Laboratory for Physical Science at Microscale, University of Science and Technology of China, Hefei, Anhui 230026, P. R. China

[‡]Key Laboratory of Materials Physics, Institute of Solid State Physics, Chinese Academy of Sciences, Hefei, Anhui 230031, P. R. China

[§]School of Materials Science and Engineering, Wuhan University of Technology, Wuhan, Hubei 430070, P. R. China

Supporting Information

ABSTRACT: Controlling the synthesis of atomic-thick nanosheets of nonlayered materials is extremely challenging because of the lack of an intrinsic driving force for anisotropic growth of two-dimensional (2D) structures. In that case, control of the anisotropy such as oriented attachment of small building blocks during the reaction process will be an effective way to achieve 2D nanosheets. Those atomic-thick nanosheets possess novel electronic structures and physical properties compared with the corresponding bulk samples. Here we report Co_9Se_8 single-crystalline nanosheets with atomic thickness and unique lamellar stacking formed by 2D oriented attachment. The atomic-thick Co_9Se_8 nanosheets were found to exhibit intrinsic half-metallic ferromagnetism, as supported by both our experimental measurements and theoretical calculations. This work will not only open a new door in the search for new half-metallic ferromagnetic systems but also pave a practical way to design ultrathin, transparent, and flexible paperlike spintronic devices.

Atomic-thick two-dimensional (2D) nanosheets have attracted tremendous attention because of their novel electronic structures and physical properties compared with the corresponding bulk samples as a result of the 2D confinement effect.[1−4] These 2D nanosheets are the most promising building blocks for the design of ultrathin, transparent, and flexible paperlike devices for their effective connecting of microscopic and macroscopic processes.[5,6] For example, the one-atomic-thick carbon nanosheet, graphene, has been applied in transparent conducting electrodes, field-effect transistors, supercapacitors, and so on.[7−9] Beyond the practical application of graphene-based devices, the interesting physical properties of graphene, such as the quantum Hall effect and half-metallicity,[10,11] are also very important for their theoretical value. Inspired by those intriguing properties of graphene, many efforts have been devoted to synthesizing free-floating 2D nanosheets of various materials with atomic thickness, including metal oxides, hydroxides, and transition-metal chalcogenides,[12−17] and then their unique electronic structures and physical properties have been primarily investigated. To date, atomic-thick 2D nanosheets are mainly produced through an exfoliation or peeling-off process based on the intrinsic layered structure characteristic of their bulk counterparts,[16] which definitely hinders further study of 2D materials. Expanding the study area to 2D nanosheets with nonlayered crystal structures is extremely urgent.

As is known, transition-metal chalcogenides possess remarkable electronic structures and physical properties, such as superconductivity, ferromagnetism, and half-metallicity, and have been systemically studied in recent years.[18−20] Reducing the dimension of bulk transition-metal chalcogenides to 2D confined nanosheets will spark new scientific interest and practical applications, such as the recently reported single-layer MoS_2-based transistor, few-layer VS_2 in-plane supercapacitors, the few-layer topological insulator Bi_2Se_3 with opening energy gap, and so on.[3,4,6]

Herein we report on the large-scale synthesis of ultrathin Co_9Se_8 nanosheets by a 2D oriented attachment strategy, which was supported by a detailed time-dependent morphology evolution study. In the ultrathin Co_9Se_8 nanosheets, four covalently bonded atomic sheets make up one quadruple layer, which is just the thickness of half a unit cell of the cubic Co_9Se_8 crystal structure. Each quadruple layer vertically stacks layer-by-layer and forms the unique lamellar structure of the synthetic ultrathin Co_9Se_8 nanosheets. The X-ray diffraction (XRD) pattern clearly shows the cubic Co_9Se_8 structure of the product with a lattice parameter of a = 10.43 Å [Figure S1a in the Supporting Information (SI)]. Energy-dispersive spectroscopy (EDS) analysis of the synthetic Co_9Se_8 nanosheets showed that the nanosheets are mainly composed of Co and Se without any impurity, with a Co/Se molar ratio of ∼1.07:1 (Figure S1b), which is close to the stoichiometric ratio of Co_9Se_8.

Figure 1a shows a transmission electron microscopy (TEM) image of the obtained product, from which one can see that the free-floating nanosheets are hundreds of nanometers in length and have flexible character. The well-defined Tyndall effect of a transparent solution of ultrathin Co_9Se_8 nanosheets (Figure 1c) indicates the presence of highly monodisperse ultrathin nanosheets in ethanol. The suspension was very stable, and no aggregation was observed upon standing for more than one month. The thickness of the as-obtained Co_9Se_8 nanosheets was measured by tapping-mode atomic force microscopy (AFM) (Figure 1b). It is amazing that the thickness of a single layer of the synthetic nanosheet is only ∼0.5 nm, which is

Received: May 14, 2012
Published: July 10, 2012

   dx.doi.org/10.1021/ja3046603 | J. Am. Chem. Soc. 2012, 134, 11908−11911

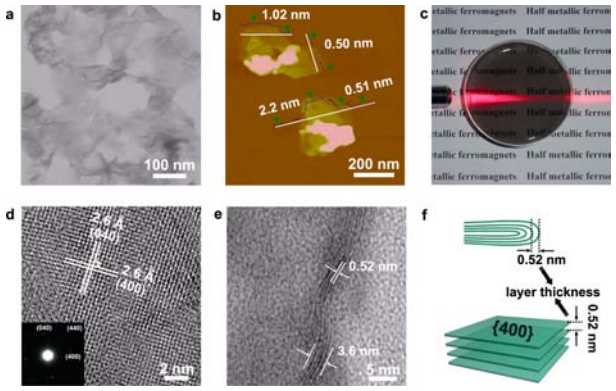

Figure 1. (a) TEM image of Co_9Se_8 ultrathin nanosheets. (b) Tapping-mode AFM image of Co_9Se_8 ultrathin nanosheets. (c) Tyndall effect of the synthetic ultrathin nanosheets dispersed in ethanol solution. (d) HRTEM image and (inset) corresponding SAED pattern of a typical Co_9Se_8 nanosheet. (e) HRTEM image of the folded edge of an ultrathin nanosheet. (f) Schematic illustration of the lamellar stacking of the synthetic nanosheets.

comparable to the thickness of graphene. The ~1.0 and ~2.2 nm heights of the stacked nanosheets (Figure 1b) can be ascribed to the thicknesses of two-layer and four-layer nanosheets, respectively. In addition, a layer thickness of ~0.52 nm was also directly determined from the high-resolution TEM (HRTEM) image of the folded edge of a nanosheet (Figure 1e), consistent with the AFM measurement. It is worth noting that the layer thickness of ~0.52 nm for a Co_9Se_8 nanosheet equals half of its unit cell parameter. The direct observation also shows that lamellar stacking of the ultrathin Co_9Se_8 nanosheets is totally different from that of other reported ultrathin nanosheets derived from materials with nonlayered crystal structures.[12,13] The synthetic nanosheets with lamellar stacking vary from single layer to several layers (Figure S4). The detailed HRTEM image of a typical nanosheet and the corresponding selected-area electron diffraction (SAED) pattern shown in Figure 1d reveal the single-crystalline nature of the nanosheet. The lattice fringes of 2.6 Å correspond to the {400} lattice plane of the Co_9Se_8 crystal structure, indicating that the ultrathin nanosheets expose the *XY* plane and should be stacked layer-by-layer along the *Z* axis. The SAED pattern (Figure 1d inset) can be indexed to fourfold symmetry along the [001] zone axis projection, confirming that the lamellar stacking of Co_9Se_8 nanosheets is along the *Z* axis in accordance with the HRTEM analysis.

These results clearly demonstrated that ultrathin Co_9Se_8 nanosheets with atomic thickness and unique lamellar stacking were successfully obtained. The flexible ultrathin nanosheets can easily be assembled into large-area films for further practical applications (section S3 in the SI). A film of ultrathin Co_9Se_8 nanosheets was obtained by a vacuum-filtration method and transferred to a transparent plastic substrate, and the thickness of the film could be controlled well by tuning the amount of Co_9Se_8 nanosheet solution used, as illustrated in detail in Figure S5. The Co_9Se_8 nanosheets on plastic substrates exhibited outstanding structural integrity and flexibility. The unique optical and mechanical properties of ultrathin Co_9Se_8 nanosheets make these nanosheets a promising candidate for the design of ultrathin, transparent, and flexible paperlike electronic devices.

The time-dependent morphology evolution was followed to study the formation mechanism of the ultrathin Co_9Se_8 nanosheets with atomic thickness and unique lamellar stacking. In the initial stage (Figure 2a), the formed small 2D nanoplates

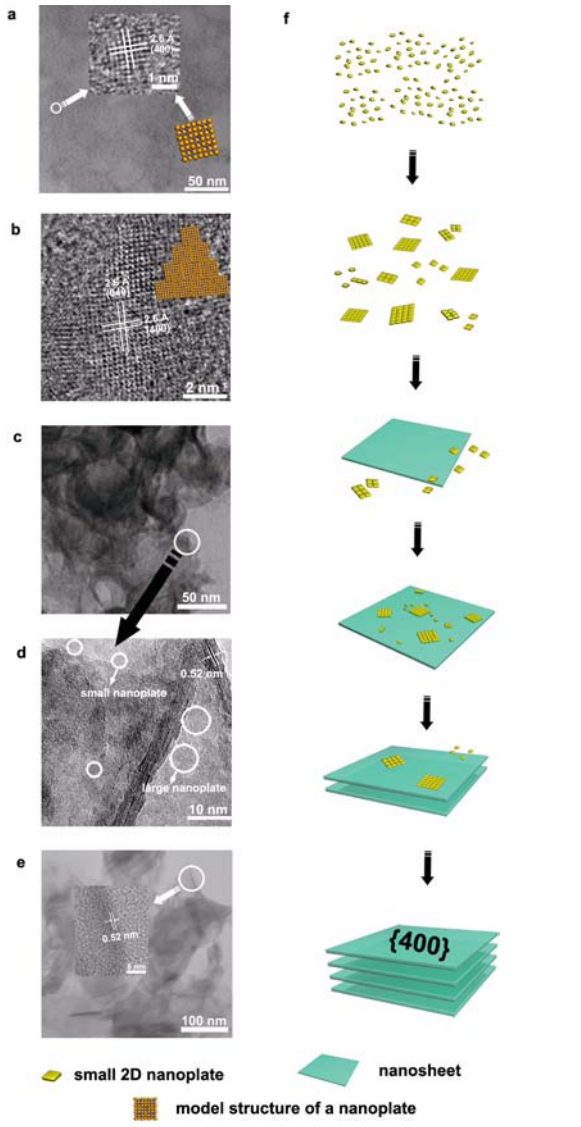

Figure 2. (a–e) TEM and HRTEM images of the intermediate product at different reaction times: (a) 0.5 h; (b) 1 h; (c, d) 5 h; (e) 15 h. (f) Schematic illustration of the time-dependent morphology evolution process for the formation of ultrathin nanosheets and their lamellar stacking.

with diameters of ~2 nm and exposed {400} planes are randomly dispersed without obvious orientation. As the reaction proceeds, the small 2D nanoplates undergo an oriented attachment process to minimize their high surface energy, forming large 2D nanoplates (Figure 2b).[21] As the oriented attachment process goes on, the 2D nanoplates ultimately evolve into large-area 2D nanosheets. When the reaction was performed for ~5 h (Figure 2c,d), 2D nanoplates became attached to the previously formed nanosheets. Those 2D nanoplates act as new nuclei for further 2D attachment, and the lamellar stacking nanosheets are formed at last (Figure 2e). Furthermore, the IR spectrum and small-angle XRD pattern (Figure S6) demonstrate the intrinsic lamellar stacking structure of the synthetic Co_9Se_8 nanosheets, excluding the influence of solvent molecules on the lamellar structure.

dx.doi.org/10.1021/ja3046603 | J. Am. Chem. Soc. 2012, 134, 11908–11911

To explore the electronic structure of the synthetic Co_9Se_8 nanosheets with atomic thickness, we carried out first-principles density functional theory (DFT) calculations. Initially, on the basis of the ~0.5 nm thickness of a Co_9Se_8 single layer from our experiment, we built a four-atomic-layer Co−Se slab model, which is just half of a unit cell of the Co_9Se_8 crystal structure (Figure 3a,b). In our slab model, four covalently bonded atomic

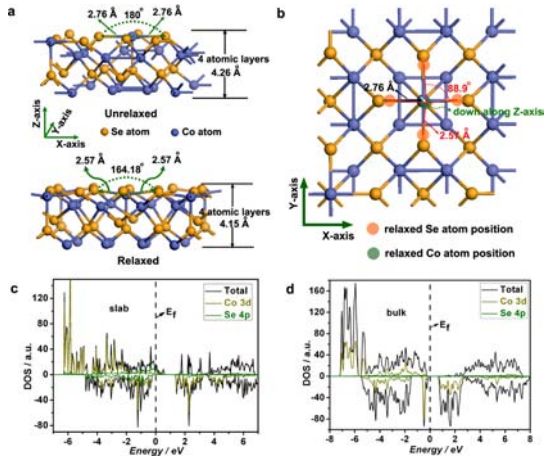

Figure 3. (a) Side view of the (top) unrelaxed and (bottom) relaxed four-atomic-layer Co_9Se_8 slab structure. (b) Structural differences between the unrelaxed and relaxed slab models. (c) Calculated DOSs of the relaxed Co_9Se_8 slab. The DOSs above zero correspond to the spin-up states, and the other to the spin-down states. (d) DOSs of bulk Co_9Se_8.

sheets make up one quadruple layer, which is considered as a repeat unit of the Co_9Se_8 crystal structure (Figure S7). What's more, this slab possesses a Co/Se atom ratio of 9:8, just matching the stoichiometric ratio of the Co_9Se_8 crystal structure. After full relaxation, the Co atoms at the surface moved downward relative to the initial Co−Se plane in the unrelaxed structure. As a result, the Co−Se bonds lengths shrink from 2.76 to 2.57 Å. Overall, such surface distortion stabilizes the slab structure and leads to a volume shrinkage of the slab at last.

Figure 3c displays the calculated density of states (DOSs) of the four-atomic-layer Co−Se slab. The curves for the spin-down states show a band gap of ~1.5 eV, whereas the curves for the spin-up states exhibit gapless. This strongly indicates that the atomic-thick nanosheet has a half-metallic nature. Furthermore, our calculations revealed that the metallic feature in the spin-up DOSs actually originates from the Co 3d and Se 4p states. For comparison, the spin-polarized DOSs of bulk Co_9Se_8 were also computed (Figure 3d). Clearly, unlike the case of the nanosheets, bulk Co_9Se_8 is a semiconductor. The calculations above strikingly indicate that reduction of the bulk Co_9Se_8 to the atomic-thick 2D nanosheet significantly alters the conductive nature from the semiconducting to half-metallic ferromagnetic. This makes the ultrathin Co_9Se_8 nanosheets with atomic thickness an ideal candidate for the design of spintronic devices.[22]

Cobalt chalcogenides are known to have excellent catalytic properties and often adsorb O atoms in their active sites if oxygen is available.[23] Thus, we handled the cases of oxygen adsorption with different concentrations on the nanosheet at the DFT level (section S9). These calculations indicated that the adsorption of external O atoms not only stabilize the Co_9Se_8 slab but also show a negligible influence on the intrinsic half-metallic ferromagnetism of the atomic-thick Co_9Se_8 nanosheets.

To support the half-metallic feature mentioned above, the electrical transport property of the synthetic Co_9Se_8 nanosheets was measured experimentally from the temperature dependence of the resistivity. As shown in Figure 4a, over the

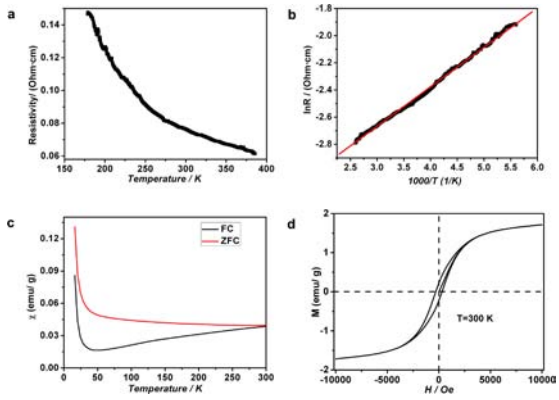

Figure 4. (a) Temperature dependence of resistivity of the synthetic ultrathin Co_9Se_8 nanosheets. (b) ln R against the reciprocal temperature of the synthetic sample, calculated from the temperature dependence of resistivity. The red line represents the best fit to the data. (c) Temperature dependence of ZFC and FC magnetization of the synthetic nanosheets. (d) Magnetic-field dependence of magnetization curve of the synthetic nanosheets at 300 K.

temperature range 380−180 K, the resistivity of the sample slightly increased with decreasing temperature. This is similar to semiconducting behavior. However, over the entire 200 K temperature range, the measured resistivity changed by a factor of only ~2.3 (from 0.063 Ω·cm at 380 K to 0.146 Ω·cm at 180 K), which is much different from typical semiconducting behavior, as the magnitude of the resistivity for a typical semiconductor should vary by several orders over such a large temperature span.[24] Thus, the observed data in Figure 4a do not strongly demonstrate the nanosheets to be semiconducting. We suggest that the weak semiconducting behavior shown in Figure 4a just reflects the half-metallic nature of the nanosheet. In fact, for the half-metallic ultrathin Co_9Se_8 nanosheets, the behaviors of the temperature-dependent resistivities of the spin-up metallic states and the spin-down semiconducting states are competitive with each other. Consequently, the sample exhibits semiconducting character with the resistivity changing by only a small factor over the concerned temperature window.

To go further, the measured resistivity was fitted as a function of $1/T$ according to the Arrhenius-type expression $R = R_o \exp(-E_a/kT)$, where R is the electrical conductivity, R_o is the pre-exponential factor, k is the Boltzmann constant, and E_a is the activation energy. The experimental data agree well with the Arrhenius law over the whole temperature range (Figure 4b), which implies that the thermal activation model would be suitable for describing the electrical transport behavior of the ultrathin Co_9Se_8 nanosheets.[25]

The temperature dependence of the zero-field-cooled (ZFC) and field-cooled (FC) magnetization and the magnetic field dependence of the magnetization ($M-H$ curve) were measured to study the magnetic properties of the ultrathin Co_9Se_8 nanosheets. The ZFC and FC curves exhibit divergence even at room temperature (Figure 4c), indicating the room-

dx.doi.org/10.1021/ja3046603 | J. Am. Chem. Soc. 2012, 134, 11908−11911

temperature ferromagnetism of Co_9Se_8 nanosheets. Further evidence for the room-temperature ferromagnetism was provided by the $M-H$ curve of the Co_9Se_8 nanosheets at 300 K (Figure 4d), which shows a coercivity (H_c) of ~300 Oe and a saturation magnetic moment (M_s) of ~1.7 emu/g, indicating that the Co_9Se_8 nanosheets are robust ferromagnets. The spin-polarization DFT calculation results showed intrinsic ferromagnetism of the Co_9Se_8 nanosheets (section S7), supporting the half-metallic ferromagnetism of ultrathin Co_9Se_8 nanosheets with atomic thickness.

In recent years, a few low-dimensional materials have been theoretically predicted to exhibit half-metallicity.[11,26−29] Some of these would present intrinsic half-metallicity but are hard to fabricate, while the others would present nonintrinsic half-metallicity derived from vacancies or doped elements in specific lattice sites; none of them have been demonstrated experimentally. To the best of our knowledge, the ultrathin Co_9Se_8 nanosheets with atomic thickness are the first artificial inorganic 2D nanosheets with intrinsic half-metallic ferromagnetism, which should attract more attention to the electronic structures and physical properties of low-dimensional transition-metal chalcogenides and offer a new direction in the search for new half-metallic materials. The intrinsic half-metallic ferromagnetism in the atomic-thick Co_9Se_8 nanosheets may begin to meet the demand for the design of ultrathin, transparent, and flexible paperlike spintronic devices.

In summary, ultrathin Co_9Se_8 nanosheets with atomic thickness and unique lamellar stacking have been synthesized by 2D oriented attachment, as supported by studies of the time-dependent morphology evolution. Both the AFM and HRTEM studies showed that the layer thickness of the synthetic Co_9Se_8 nanosheets is ~0.52 nm, which is just half of a unit cell of the cubic Co_9Se_8 crystal structure. The ultrathin Co_9Se_8 nanosheets can be easily assembled into transparent and flexible films for further practical applications. The intrinsic half-metallic ferromagnetism in the atomic-thick Co_9Se_8 nanosheets was predicted by theoretical DFT calculations and experimentally supported by electrical transport and magnetic studies. The half-metallic ferromagnetism in the synthetic ultrathin Co_9Se_8 nanosheets with atomic thickness will not only inspire scientific interest in the possible half-metallic ferromagnetism of low-dimensional materials but also pave a practical way to achieve ultrathin, transparent, and flexible paperlike spintronic devices.

■ ASSOCIATED CONTENT

Supporting Information

Detailed experimental section, characterization and calculation methods, and additional material characterization. This material is available free of charge via the Internet at http://pubs.acs.org.

■ AUTHOR INFORMATION

Corresponding Author

yxie@ustc.edu.cn

Notes

The authors declare no competing financial interest.

■ ACKNOWLEDGMENTS

The research was financially supported by the National Basic Research Program of China (2009CB939901) and the National Natural Science Foundation of China (11079004, 10979047, and 90922016).

■ REFERENCES

(1) Novoselov, K. S.; Jiang, D.; Schedin, F.; Booth, T. J.; Khotkevich, V. V.; Morozov, S. V.; Geim, A. K. *Proc. Natl. Acad. Sci. U.S.A.* **2005**, *102*, 10451.

(2) Novoselov, K. S. *Rev. Mod. Phys.* **2011**, *83*, 837.

(3) Radisavljevic, B.; Radenovic, A.; Brivio, J.; Giacometti, V.; Kis, A. *Nat. Nanotechnol.* **2011**, *6*, 147.

(4) Zhang, Y.; He, K.; Chang, C.-Z.; Song, C.-L.; Wang, L.-L.; Chen, X.; Jia, J.-F.; Fang, Z.; Dai, X.; Shan, W.-Y.; Shen, S.-Q.; Niu, Q.; Qi, X.-L.; Zhang, S.-C.; Ma, X.-C.; Xue, Q.-K. *Nat. Phys.* **2010**, *6*, 584.

(5) Pushparaj, V. L.; Shaijumon, M. M.; Kumar, A.; Murugesan, S.; Ci, L.; Vajtai, R.; Linhardt, R. J.; Nalamasu, O.; Ajayan, P. M. *Proc. Natl. Acad. Sci. U.S.A.* **2007**, *104*, 13574.

(6) Feng, J.; Sun, X.; Wu, C. Z.; Peng, L. L.; Lin, C. W.; Hu, S. L.; Yang, J. L.; Xie, Y. *J. Am. Chem. Soc.* **2011**, *133*, 17832.

(7) Wang, X.; Zhi, L.; Müllen, K. *Nano Lett.* **2007**, *8*, 323.

(8) Meric, I.; Han, M. Y.; Young, A. F.; Ozyilmaz, B.; Kim, P.; Shepard, K. L. *Nat. Nanotechnol.* **2008**, *3*, 654.

(9) Zhu, Y.; Murali, S.; Stoller, M. D.; Ganesh, K. J.; Cai, W.; Ferreira, P. J.; Pirkle, A.; Wallace, R. M.; Cychosz, K. A.; Thommes, M.; Su, D.; Stach, E. A.; Ruoff, R. S. *Science* **2011**, *332*, 1537.

(10) Zhang, Y.; Tan, Y.-W.; Stormer, H. L.; Kim, P. *Nature* **2005**, *438*, 201.

(11) Son, Y.-W.; Cohen, M. L.; Louie, S. G. *Nature* **2006**, *444*, 347.

(12) Schliehe, C.; Juarez, B. H.; Pelletier, M.; Jander, S.; Greshnykh, D.; Nagel, M.; Meyer, A.; Foerster, S.; Kornowski, A.; Klinke, C.; Weller, H. *Science* **2010**, *329*, 550.

(13) Son, J. S.; Wen, X.-D.; Joo, J.; Chae, J.; Baek, S.-i.; Park, K.; Kim, J. H.; An, K.; Yu, J. H.; Kwon, S. G.; Choi, S.-H.; Wang, Z.; Kim, Y.-W.; Kuk, Y.; Hoffmann, R.; Hyeon, T. *Angew. Chem., Int. Ed.* **2009**, *48*, 6861.

(14) Yu, T.; Lim, B.; Xia, Y. *Angew. Chem., Int. Ed.* **2010**, *49*, 4484.

(15) Min, Y.; Moon, G. D.; Kim, B. S.; Lim, B.; Kim, J.-S.; Kang, C. Y.; Jeong, U. *J. Am. Chem. Soc.* **2012**, *134*, 2872.

(16) Coleman, J. N.; Lotya, M.; O'Neill, A.; Bergin, S. D.; King, P. J.; Khan, U.; Young, K.; Gaucher, A.; De, S.; Smith, R. J.; Shvets, I. V.; Arora, S. K.; Stanton, G.; Kim, H.-Y.; Lee, K.; Kim, G. T.; Duesberg, G. S.; Hallam, T.; Boland, J. J.; Wang, J. J.; Donegan, J. F.; Grunlan, J. C.; Moriarty, G.; Shmeliov, A.; Nicholls, R. J.; Perkins, J. M.; Grieveson, E. M.; Theuwissen, K.; McComb, D. W.; Nellist, P. D.; Nicolosi, V. *Science* **2011**, *331*, 568.

(17) Ma, R.; Sasaki, T. *Adv. Mater.* **2010**, *22*, 5082.

(18) Hsu, F.-C.; Luo, J.-Y.; Yeh, K.-W.; Chen, T.-K.; Huang, T.-W.; Wu, P. M.; Lee, Y.-C.; Huang, Y.-L.; Chu, Y.-Y.; Yan, D.-C.; Wu, M.-K. *Proc. Natl. Acad. Sci. U.S.A.* **2008**, *105*, 14262.

(19) Kwon, S. K.; Youn, S. J.; Min, B. I. *Phys. Rev. B* **2000**, *62*, 357.

(20) Xie, W.-H.; Xu, Y.-Q.; Liu, B.-G.; Pettifor, D. G. *Phys. Rev. Lett.* **2003**, *91*, No. 037204.

(21) Lee, E. J. H.; Ribeiro, C.; Longo, E.; Leite, E. R. *J. Phys. Chem. B* **2005**, *109*, 20842.

(22) Wolf, S. A.; Awschalom, D. D.; Buhrman, R. A.; Daughton, J. M.; von Molnár, S.; Roukes, M. L.; Chtchelkanova, A. Y.; Treger, D. M. *Science* **2001**, *294*, 1488.

(23) Gao, M. R.; Jiang, J.; Yu, S. H. *Small* **2012**, *8*, 13.

(24) Tengå, A.; Lidin, S.; Belieres, J.-P.; Newman, N.; Wu, Y.; Häussermann, U. *J. Am. Chem. Soc.* **2008**, *130*, 15564.

(25) McMillan, W. L. *Phys. Rev. B* **1983**, *28*, 5216.

(26) Kan, E. J.; Hu, W.; Xiao, C. Y.; Lu, R. F.; Deng, K. M.; Yang, J. L.; Su, H. B. *J. Am. Chem. Soc.* **2012**, *134*, 5718.

(27) Wang, L.; Cai, Z.; Wang, J.; Lu, J.; Luo, G.; Lai, L.; Zhou, J.; Qin, R.; Gao, Z.; Yu, D.; Li, G.; Mei, W. N.; Sanvito, S. *Nano Lett.* **2008**, *8*, 3640.

(28) Kan, E.-J.; Wu, X.; Li, Z.; Zeng, X. C.; Yang, J.; Hou, J. G. *J. Chem. Phys.* **2008**, *129*, No. 084712.

(29) Chen, Q.; Wang, J. L.; Zhu, L. Y.; Wang, S. D.; Ding, F. *J. Chem. Phys.* **2010**, *132*, No. 204703.